NANO LETTERS

Letter

pubs.acs.org/NanoLett

Hierarchical Three-Dimensional $ZnCo_2O_4$ Nanowire Arrays/Carbon Cloth Anodes for a Novel Class of High-Performance Flexible Lithium-Ion Batteries

Bin Liu,[†] Jun Zhang,[†] Xianfu Wang,[†] Gui Chen,[†] Di Chen,*[,†] Chongwu Zhou,*[,‡] and Guozhen Shen*[,†]

[†]Wuhan National Laboratory for Optoelectronics and College of Optoelectronic Science and Engineering, Huazhong University of Science and Technology, Wuhan 430074, China

[‡]Department of Electric Engineering, University of Southern California, Los Angeles, California 90089, United States

Supporting Information

ABSTRACT: Flexible electronics is an emerging and promising technology for next generation of optoelectronic devices. Herein, hierarchical three-dimensional $ZnCo_2O_4$ nanowire arrays/carbon cloth composites were synthesized as high performance binder-free anodes for Li-ion battery with the features of high reversible capacity of 1300−1400 mAh g^{-1} and excellent cycling ability even after 160 cycles with a capacity of 1200 mAh g^{-1}. Highly flexible full batteries were also fabricated, exhibiting high flexibility, excellent electrical stability, and superior electrochemical performances.

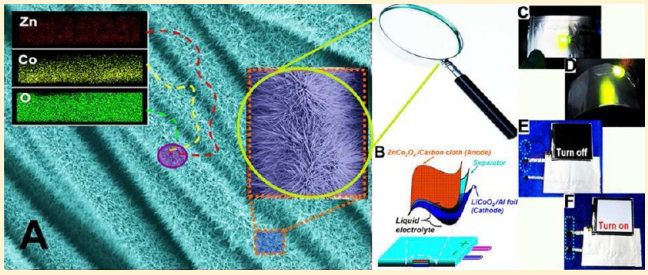

KEYWORDS: *Energy storage, flexible electronics, hierarchical 3D $ZnCo_2O_4$ arrays, high-performance lithium-ion batteries*

Flexible/bendable electronics is an emerging and promising technology for the next generation of optoelectronic devices in various applications such as rollup displays, smart electronics, and wearable devices.[1−6] In particular, recent progress in the study of new inexpensive, flexible, lightweight, and environmentally friendly energy storage devices has triggered a gold rush for exploiting their higher performance.[7−20] Though several kinds of flexible substrates in the composite electrodes has been reported,[21−23] it is still a great challenge to fabricate highly flexible energy storage devices with high mechanical strength and excellent electrical stability.

$ZnCo_2O_4$ has been considered as an attractive candidate for substitution of the conventional graphite anode in lithium ion battery due to its superiorities such as improved reversible capacities, enhanced cycling stability, and good environmental benignity.[24−27] Until now, nanoparticles and porous nanoflakes of $ZnCo_2O_4$ has been synthesized to be used as anode for Li-ion battery with good first-cycle reversible capacity. However, the simple structures, poor electric conductivity, and large volume change of the $ZnCo_2O_4$ nanostructures during the electrochemical reaction led to fast capacity decrease. Very recently, there-dimensional (3D) hierarchical architectures with large surface areas, better permeabilities, and more active sites have been reported with potential applications in optoelectronic devices, catalysts, supercapacitors, and lithium ion batteries.[28−36] It is expected that advancements in lithium ion battery technology can be achieved by combining both flexible design approach and hierarchical 3D nanostructures in a complete battery configuration.[37]

In this work, we report the synthesis of unique hierarchical 3D $ZnCo_2O_4$ nanowire arrays/carbon cloth exhibiting high capacity, excellent cycling performance, and good rate capability. By using the hierarchical 3D $ZnCo_2O_4$ nanowire arrays/carbon cloth as both a new class of binder-free anode and the current collectors to replace traditional 2D metal current collectors such as copper, aluminum, highly flexible lithium rechargeable batteries with excellent mechanical strength and superior electrochemical performance were fabricated, which can be used to control commercial available LED and displays.

The 3D $ZnCo_2O_4$ nanowire arrays with high density could be easily grown on the carbon cloth by using a facile hydrothermal route. The mass of the nanowires were determined by cutting the carbon cloth with grown samples into smaller pieces with the diameter of 13 mm. Then both the carbon cloth with grown samples and carbon cloth were weighed with a high-precision analytical balance (Sartorius, max weight 5100 mg, d = 0.001 mg) from which the exact mass of the samples was then determined. The loading density of the $ZnCo_2O_4$ active material is calculated as 0.3−0.6 mg/cm^2. The growth process was illustrated in Figure 1a. The structure of the as-synthesized hierarchical $ZnCo_2O_4$ nanowire arrays/carbon cloth was characterized by the SEM technique, as shown in Figure 1. Figure 1b clearly displays the well-established texture structure of the $ZnCo_2O_4$ nanowire arrays grown on the carbon fiber

Received: February 27, 2012
Revised: May 12, 2012
Published: May 18, 2012

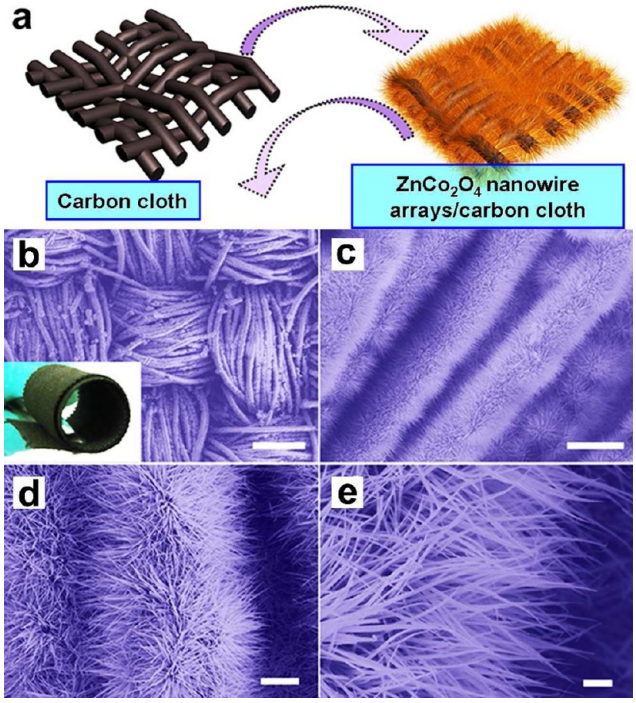

Figure 1. (a) Schematic illustration of the synthesis of flexible 3D $ZnCo_2O_4$ nanowire arrays/carbon cloth. Morphology characterization. (b–e) Typical FESEM images of the $ZnCo_2O_4$ nanowire arrays growing on carbon cloth at different magnifications. (Inset in panel b) Photographic image of product exhibited very good flexibility and it can be rolled up periodically with a tweezer. Scale bars, 200 μm (b); 20 μm (c); 5 μm (d); 1 μm (e).

cloth. The final product still keeps the ordered woven structure of the carbon cloth templates (Supporting Information Figure S1). The inset in Figure 1b shows a photographic image of the $ZnCo_2O_4$/carbon cloth composite, exhibiting excellent flexibility. It can be readily rolled up periodically with a tweezer, making it possible for further flexible device applications. Higher-magnification SEM images shown in Figure 1c–e provide clearer information about the final products. From Figure 1c, we can see that each $ZnCo_2O_4$ nanowire arrays/carbon composite fibers has uniform diameter of approximately 20 μm. Each composite fiber composed of numerous highly ordered novel 3D $ZnCo_2O_4$ arrays with relatively high nanowire density grown on an individual carbon microfiber, as can be seen from Figure 1d and Supporting Information Figure S2. Typical $ZnCo_2O_4$ nanowires have uniform diameters of about 80–100 nm and lengths of about 5 μm.

Further information about the $ZnCo_2O_4$ nanowires was obtained from transmission electron microscopy (TEM). Figure 2a shows the low-magnification TEM image, where nanowires with diameters of about 80–100 nm can be clearly seen. A higher-magnification TEM image depicted in Figure 2b–d reveals that a typical $ZnCo_2O_4$ nanowire is actually a porous nanowire composed of many small nanoparticles instead of the conventional single-crystalline nanowire. The HRTEM image shown in Figure 2c reveals two sets of lattice fringes with interplane spacings of 0.29 and 0.25 nm, respectively, corresponding to the (220) and (311) planes of spinel $ZnCo_2O_4$ phase. The crystallographic structure of the product was further analyzed by X-ray diffraction (XRD) as shown in Figure 2e. All the diffraction peaks in this pattern can be readily indexed as spinel $ZnCo_2O_4$, which are consistent with the values in the standard card (JCPDS Card No. 23-1390). Besides, the peaks at around 26 and 43° were also observed, coming from the carbon cloth templates. The crystal structure of spinel $ZnCo_2O_4$ is demonstrated in the inset of Figure 2e. The cubic lattice parameter, space group ($Fd3m$) is evaluated by the least-squares fitting of 2θ and (hkl). The triangular pyramids (blue), octahedrons (purple), and small spheres (red) represent Zn atoms, Co atoms, and O atoms, respectively. Energy dispersive spectroscopy (EDS) microanalysis of the $ZnCo_2O_4$ nanowires was shown in Figure 2f. The entire nanostructures were found to consist of only Zn, Co, and O elements, further indicating the formation of pure $ZnCo_2O_4$. Energy dispersive X-ray spectroscopy mapping shown in Figure 2g provides clearer information about the element distribution within the nanowires, which further confirm the formation of pure $ZnCo_2O_4$ products.

The electrochemical properties of the as-synthesized hierarchical $ZnCo_2O_4$ nanowire arrays/carbon cloth electrodes were measured by configuring them as the laboratory-based

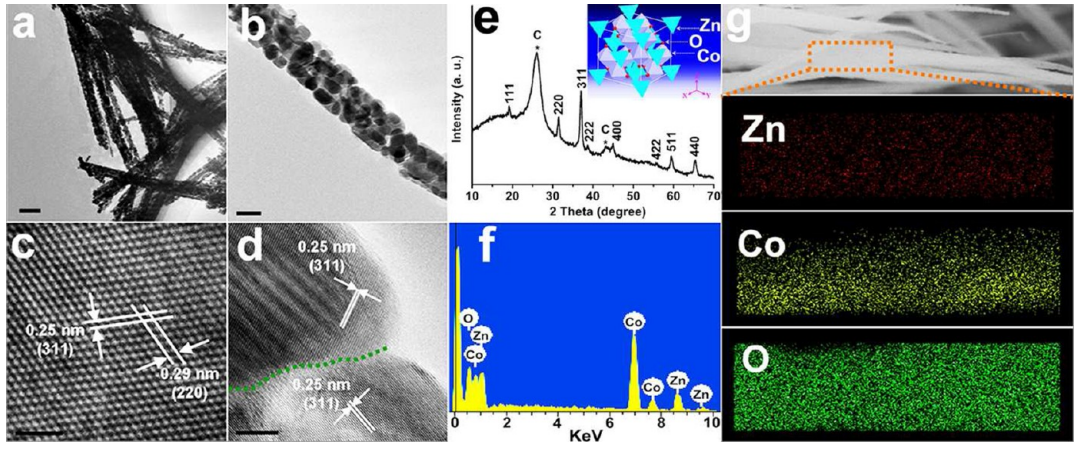

Figure 2. Phase analysis. (a–d) TEM and high-resolution TEM images of hierarchical $ZnCo_2O_4$ nanowires. (e) XRD pattern of $ZnCo_2O_4$/C composite. The inset of (e) is the crystal structure of cubic spinel $ZnCo_2O_4$. (f) The EDS microanalysis on selected areas. (g) SEM image and corresponding EDX elemental mappings of Zn, Co, and O for the $ZnCo_2O_4$ nanowire arrays. Scale bars, 200 nm (a); 50 nm (b); 2 nm (c); 5 nm (d).

dx.doi.org/10.1021/nl300794f | *Nano Lett.* 2012, 12, 3005–3011

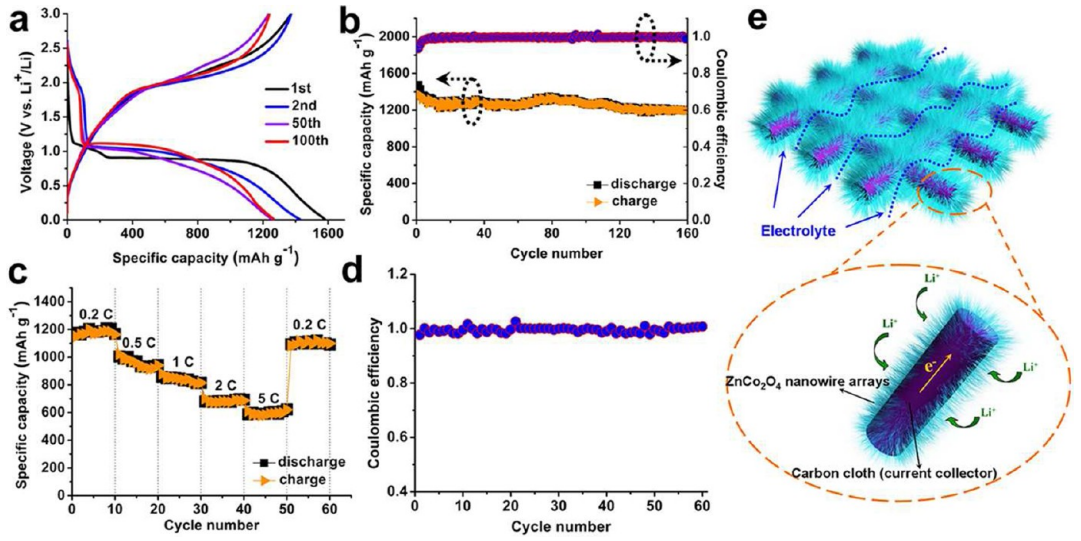

Figure 3. Electrochemical characterizations. (a) Typical voltage versus specific capacity profiles for the first first, second, 50th, and 100th discharge- and charge-cycle. (b) Long-term cycling of the $ZnCo_2O_4$ nanowire arrays/carbon cloth electrode, showing the reversible capacity value of 1200 mAh g^{-1} after 160 cycles with Coulombic efficiency of 99%. (c) Capacity versus cycle number plot at different charging rates. (d) Coulombic efficiency versus cycle number at various current rates. (e) Schematic representation and operating principles of rechargeable lithium-ion battery based on $ZnCo_2O_4$ nanowire arrays/carbon cloth.

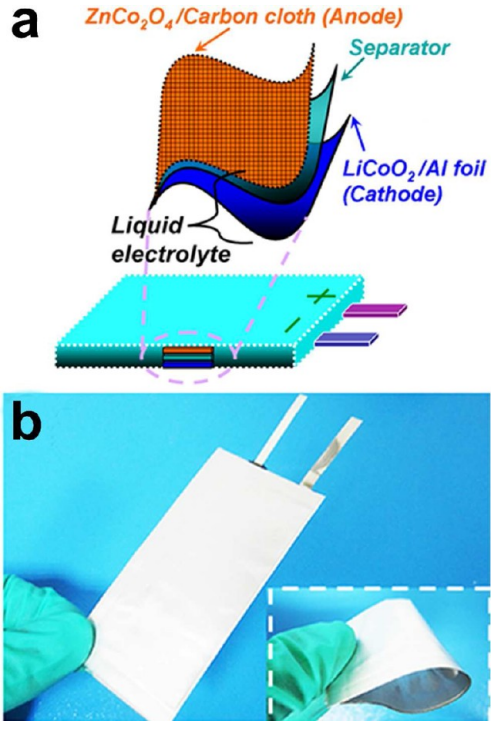

Figure 4. Schematic illustration for the fabrication of the hierarchical 3D $ZnCo_2O_4$ nanowire arrays/carbon cloth/liquid electrolyte/$LiCoO_2$ flexible lithium-ion battery. (a) Structure of the flexible Li-ion battery. (b) Digital images of the fabricated flexible Li-ion battery.

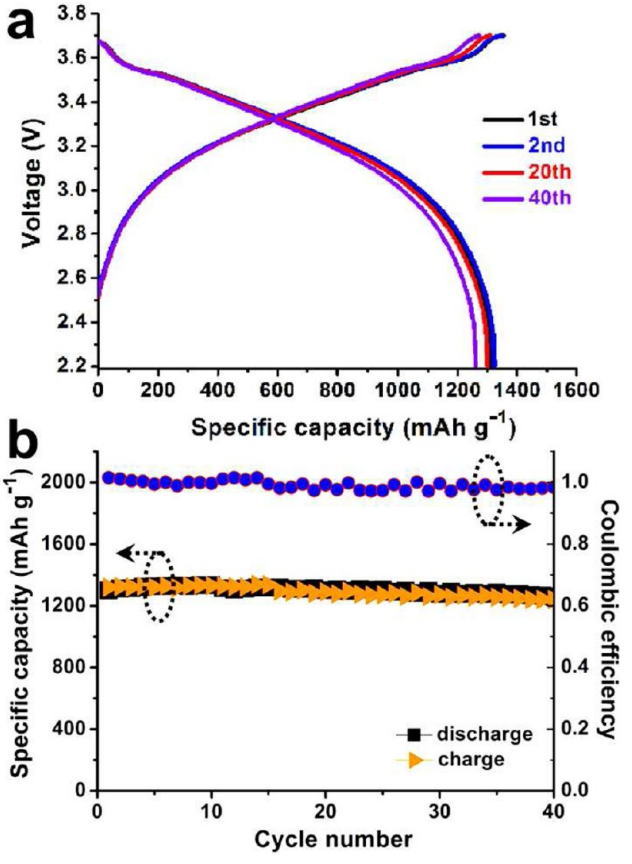

Figure 5. Electrochemical characterizations of flexible full $ZnCo_2O_4$/liquid electrolyte/$LiCoO_2$ battery. (a) Charge−discharge curves for first, second, 20th, and 40th cycles. (b) Cycling performance of flexible full battery up to 40 cycles at current density of 200 mAh g^{-1}.

CR2032 coin cell. The $ZnCo_2O_4$/carbon cloth as anode was investigated versus Li metal under galvanostatic cycling conditions at room temperature at a current rate of 200 mA g^{-1} in the voltage window of 0.01−3.0 V. Figure 3a shows the voltage-capacity profiles of the as-prepared $ZnCo_2O_4$/carbon cloth electrodes for the first, second, 50th, and 100th charge/discharge cycles, respectively. From these curves, it can be seen that all discharge curves exhibit a distinct plateau between 0.8 and 1.2 V. It should be noted that the plateau of the second, 50th, and 100th discharge curves is slightly higher than that of the first discharge curves, similar to previous reports.[22,24] The discharge capacities of the hierarchical electrode in the first,

dx.doi.org/10.1021/nl300794f | Nano Lett. 2012, 12, 3005−3011

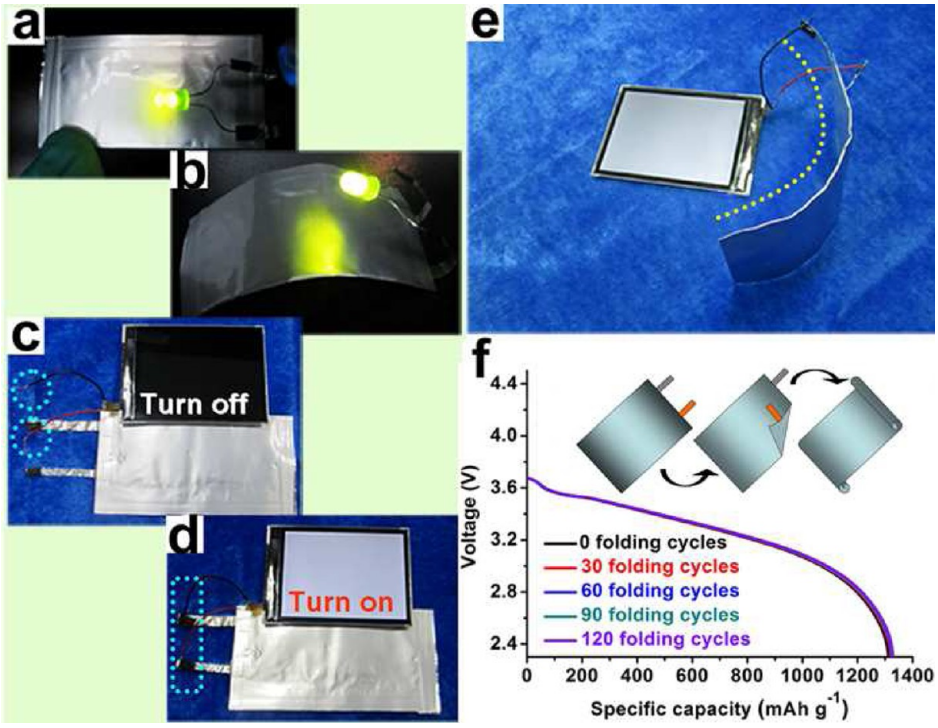

Figure 6. A flexible full battery based on $ZnCo_2O_4$/liquid electrolyte/$LiCoO_2$ displays in the practical applications and electronic stability measurement of the flexible device. (a,b) The optical images show a light-emitting-diode (LED) lighting by a free-bending and bending battery device. (c,d) The images reveal a mobile phone screen can be switched from the "OFF" state to the "ON" state by a device composed of $ZnCo_2O_4$/liquid electrolyte/$LiCoO_2$. (e) The digital photo of tuning on a mobile phone screen by a foldable battery. (f) The voltage versus specific capacity profiles of full flexible battery before and after 30, 60, 90, and 120 cycles of bending.

second, 50th, and 100th cycles are calculated to be around 1530, 1420, 1280, and 1278 mAh g^{-1}, respectively. The irreversible capacity loss for the first cycle may be attributed to the formation of solid electrolyte interphase (SEI) and reduction of metal oxide to metal with Li_2O formation, which is commonly observed for a variety of electrode materials.

Figure 3b is the discharge/charge capacities versus cycle number of the $ZnCo_2O_4$/carbon cloth at a rate of 200 mA g^{-1}. It clearly reveals that, except for the irreversible specific capacity for the first discharge (1530 mAh g^{-1}), the following charge−discharge capacities in the measured range tended to be stable and the value almost maintains constant in the range of about 1200−1340 mAh g^{-1} with 99% capacity retention from 3 to 160 cycles. It is very common that the specific capacities higher than the theoretical value were mentioned.[10,38] The increasing specific capacity for $ZnCo_2O_4$/carbon cloth electrodes may be ascribed to the reversible growth of a polymeric gel-like film resulting from kinetically activated electrolyte degradation.[39−41] To further address the issue, we checked the electrodes with TEM technique and the corresponding TEM images were depicted in Supporting Information Figure S4, revealing a reversible formation/dissolution of the polymer/gel-like film on the surface of the active materials during the discharge/charge processes. Supporting Information Figure S4a shows the formation of the polymeric gel-like film layer with size of ∼8 nm after 50th discharge and it almost disappeared after 50th charge (Supporting Information Figure S4b). Similar results were also founded by Tarascon et al et al.[38,41,42] No remarkable decay was found for the $ZnCo_2O_4$/carbon cloth electrodes and the capacity is still about 1200 mAh g^{-1} even after 160 cycles, indicating very good reversible capacity and cycling stability. The steady-going reversible capacity of 1200−1340 mAh g^{-1} obtained here during discharge/charge reactions is as long as 160 cycles at 200 mAh g^{-1}, which is much higher and more stable than the previously reported values for $ZnCo_2O_4$ materials.[24−26] Besides, the capacity of pure carbon cloth was also studied for comparison and the result was demonstrated in Supporting Information Figure S3. It reveals that pure carbon cloth exhibited quite low capacity, indicating that the capacity of carbon cloth has almost no effect to the overall capacity of $ZnCo_2O_4$ electrodes. In addition, the columbic efficiency between discharge and charge capacities was also studied and the value is as high as 99% (3−160 cycles), indicating excellent electrochemical reversibility during the lithium insertion and extraction reactions. Considering that no ancillary materials such as polymer binder and carbon black are used in the present work, the present hierarchical $ZnCo_2O_4$/carbon cloth are more suitable candidates to be used as electrodes for high performance lithium-ion batteries.

To further confirm the excellent performance of the as-synthesized $ZnCo_2O_4$/carbon cloth, the electrochemical properties of the $ZnCo_2O_4$/carbon cloth were studied by charging/discharging at different C rates ranging from 0.2 to 5 C (1C = 900 mAh g^{-1}), because rate capability is another important parameter for many practical applications of lithium ion batteries such as electric vehicles and power tools.[43] From Figure 3c, it can be see that the capacity decreases from 1200, 920, 890, 710, and 605 mAh g^{-1} with increasing C-rate ranging from 0.2, 0.5, 1, 2, to 5 C. The capacity is then reversibly back to 1105 mAh g^{-1} once the charging/discharging rate was set back to 0.2 C again, revealing that almost 92% of the initial capacity at 0.2 C was recovered. The corresponding Coulombic efficiency of the rate capability for the $ZnCo_2O_4$/carbon cloth is plotted in Figure 3d. Although different discharge/charge rates

dx.doi.org/10.1021/nl300794f | Nano Lett. 2012, 12, 3005−3011

are gradually applied, the Coulombic efficiency (>98%) is still highly expected from our samples, which further demonstrates the excellent battery performance of the $ZnCo_2O_4$/carbon cloth electrode. On the basis of the above results, the excellent cycling stability, high specific capacity, and outstanding rate performance of the current hierarchical 3D architecture of $ZnCo_2O_4$ nanowire arrays/carbon cloth make it a promising candidate for the anode material for Li-ion batteries and will be favorable for immense potential application in electrochemical energy storage. According to previous reports, the electrochemical process of the as-synthesized nanostructures can be clarified as follows

$$ZnCo_2O_4 + 8Li^+ + 8e^- \leftrightarrow Zn + 2Co + 4Li_2O \quad (1)$$

$$Zn + Li^+ + e^- \leftrightarrow LiZn \quad (2)$$

$$Zn + Li_2O \leftrightarrow ZnO + 2Li^+ + 2e^- \quad (3)$$

$$2Co + 2Li_2O \leftrightarrow 2CoO + 4Li^+ + 4e^- \quad (4)$$

$$2CoO + \frac{2}{3}Li_2O \leftrightarrow \frac{2}{3}Co_3O_4 + \frac{4}{3}Li^+ + \frac{4}{3}e^- \quad (5)$$

In order to further explain the electrochemical process, we investigated the electrode material in the fully Li-inserted state by using XRD technique and the corresponding XRD pattern is shown in Supporting Information Figure S5. All the peaks in the pattern can be indexed to Li_2O, Zn, Co, and LiF, respectively. It should be mentioned that the peaks of LiF come from the decomposition of the electrolyte ($LiPF_6$) embedded in the 3D structure in the air when doing XRD measurement. The XRD data confirm the above proposed electrochemical process of the $ZnCo_2O_4$ based Li-ion batteries.

Figure 3e shows the schematic representation and operating principles of the rechargeable lithium-ion battery based on the $ZnCo_2O_4$ /carbon cloth. The high capacity, excellent cycling stability, and good rate capability can be attributed to the unique morphology and structure of the current $ZnCo_2O_4$/carbon cloth electrodes on the following aspects: (1) The $ZnCo_2O_4$ nanowire arrays directly grown on the carbon cloth have an outstanding electronic conductivity because $ZnCo_2O_4$ nanowire arrays sticked tightly to the carbon cloth to form very good adhesion and electrical contact, building up an expressway for charge transfer. (2) The 3D configuration of the $ZnCo_2O_4$/carbon cloth ensures the loose textures and open spaces between neighboring nanowire arrays, thus greatly enhancing the electrolyte/$ZnCo_2O_4$ contact area, which provide ideal conditions for facile diffusion of the electrolyte and accommodation of the strain induced by the volume change during electrochemical reactions, thus leading to a higher efficiency of lithiation and delithiation under the electrolyte penetration. (3) Elastic feature of individual nanowire within the aligned $ZnCo_2O_4$ arrays releases the pressure imposed on them when assembling into cells, which then prevents the nanowire arrays from pulverization and fragmentation.[44] (4) The novel 3D array structure shortens the Li^+ ion diffusion paths in the nanowires and enhances the rate capability.

The as-grown $ZnCo_2O_4$/carbon cloth exhibited high capacity, excellent cycling stability, and good rate capability. By using the as-grown $ZnCo_2O_4$/carbon cloth as a binder-free anode, we further demonstrated the fabrication of flexible lithium ion full battery here. The structure of the fabricated flexible full battery was demonstrated in Figure 4a, which consists of the flexible $ZnCo_2O_4$/carbon cloth as anode, flexible separator, the $LiCoO_2$/Al foil as cathode, $LiPF_6$-based electrolyte, and flexible plastic shell. Figure 4b displays a photograph of the final packaged full battery device, which is consistent well with the schematic in Figure 4a. An inset image shown in Figure 4b reveals the excellent flexible and ultrathin like a paper feature of the device.

It is well-known that the capacity of commercial $LiCoO_2$ cathode is 40 mAh, which is much higher than the total capacity of the as-synthesized $ZnCo_2O_4$ active materials (about 20−23 mAh). Hence, the final full batteries are anode-limited and the specific capacity and rate of the batteries referred to the mass of the negative $ZnCo_2O_4$ electrodes. Figure 5a presents the voltage-capacity profiles of as-prepared flexible full battery device for the first, second, 20th, and 40th charge/discharge cycles at a current rate of 200 mA g^{-1} in the voltage window of 2.2−3.7 V. The corresponding charge/discharge curves present two plateaus and the average discharge voltage is 3.4 V, which reveals the two-stage Li ion insertion/extraction behavior. The initial irreversible discharge capacity of the hybrid electrodes is about 1314 mAh g^{-1} and the reversible discharge capacity remains stable in the following cycling, indicating good reversibility. Figure 5b shows the cycling performance of $ZnCo_2O_4$/$LiCoO_2$ battery cycled between 2.2 and 3.7 V at a current density of 200 mAh g^{-1}. It reveals that the reversible capacity of the flexible device maintains a nearly constant value of approximately 1300 mAh g^{-1} and still keeps about 96% of the initial capacity even after 40 cycles, demonstrating the high charge/discharge capacities and the excellent capacity retention. In addition, Coulombic efficiency versus cycle number for this device was also measured and it is sustained at around 97−99%.

To demonstrate its practical applications, the as-fabricated flexible full battery was used to control a commercial green LED and a LCD mobile display, even hand-held device, such as Game Boy Color (see the Video S1 in Supporting Information), as demonstrated in Figure 6a−e and Supporting Information S6. They can be easily lightened even when the battery was bended (Figure 6b,e). The folding endurance is an important parameter of flexible device. Figure 6f illustrates the typical voltage profiles of the flexible battery device by bending it from different directions for hundreds cycles. From the curves, it can be seen that the discharge capacities of the device remains almost constant even after 120 cycles of bending, revealing that the electrical stability of the fabricated flexible full battery is hardly affected by external bending stress.

In summary, we successfully synthesized hierarchical $ZnCo_2O_4$ nanowire arrays/carbon cloth exhibiting high capacity, excellent cycling stability, and good rate capability. Using the flexible $ZnCo_2O_4$ nanowire arrays/carbon cloth as anode, we fabricated a highly flexible full battery with outstanding performances in terms of capacity, rate capability, and cycle-life. It not only ensures high and stable capability to be operated under fully mechanical bending, but also superior electrochemical performances over conventional electrode architectures. Hierarchical 3D $ZnCo_2O_4$ nanowire arrays/carbon cloth as a novel class of high-performance flexible lithium ion batteries make it possible to be directly applied in various potential applications, such as stretchable/bendable electronic devices, portable energy storage devices, flexible powering sustainable vehicles, and photovoltaic devices.

dx.doi.org/10.1021/nl300794f | Nano Lett. 2012, 12, 3005−3011

■ ASSOCIATED CONTENT

Supporting Information

Experimental details of device preparations, structural characterizations, battery assembly, electrochemical measurements, additional supporting data, and the video about a Game Boy Color controlled by as-fabricated flexible lithium-ion battery. This material is available free of charge via the Internet at http://pubs.acs.org.

■ AUTHOR INFORMATION

Corresponding Author

*E-mail: (G.Z.S.) gzshen@mail.hust.edu.cn; (C.W.Z.) chongwuz@usc.edu; (D.C.) dichen@mail.hust.edu.cn.

Notes

The authors declare no competing financial interest.

■ ACKNOWLEDGMENTS

This work was supported by the National Natural Science Foundation (51002059, 21001046, 91123008), the 973 Program of China (2011CBA00703, 2011CB933300), the Program for New Century Excellent Talents of the University in China (Grant NCET-11-0179), the Research Fund for the Doctoral Program of Higher Education (20090142120059, 20100142120053), the Natural Science Foundation of Hubei Province (2011CDB035), and the Director Fund of WNLO. Special thanks to the Analytical and Testing Center of HUST and the Center of Micro-Fabrication and Characterization (CMFC) of WNLO for using their facilities. Thanks to Professor Jinping Liu, Jianming Gao, and Xiaoxia Ding at Central China Normal University as well as Professor Xianluo Hu and Dr. Yongming Sun at HUST for strong support and stimulating discussion.

■ REFERENCES

(1) Gwon, H.; Kim, H. S.; Lee, K. U.; Seo, D. H.; Park, Y. C.; Lee, Y. S.; Ahn, B. T.; Kang, K. Flexible energy storage devices based on graphene paper. *Energy Environ. Sci.* **2011**, *4*, 1277−1283.

(2) Liu, J.; Buchholz, D. B.; Chang, R. P.; Facchetti, A.; Marks, T. J. High-performance flexible transparent thin-film transistors using a hybrid gate dielectric and an amorphous zinc indium tin oxide channel. *Adv. Mater.* **2010**, *22*, 2333−2337.

(3) Lieber, C. M.; Wang, Z. L. Functional nanowires. *MRS Bull.* **2007**, *32*, 99−108.

(4) Wang, Z. R.; Wang, H.; Liu, B.; Qiu, W. Z.; Zhang, J.; Ran, S. H.; Huang, H. T.; Xu, J.; Han, H. W.; Chen, D.; Shen, G. Z. Transferable and Flexible Nanorod-Assembled TiO_2 Cloths for Dye-Sensitized Solar Cells, Photodetectors, and Photocatalysts. *ACS Nano* **2011**, *5*, 8412−8419.

(5) Duan, X. F. Assembled semiconductor nanowire thin films for high performance flexible macroelectronics. *MRS Bull.* **2007**, *32*, 134−141.

(6) Chen, P. C.; Shen, G. Z.; Chen, H.; Shi, Y.; Zhou, C. W. Preparation and Characterization of Flexible Asymmetric Supercapacitors Based on Transition-Metal-Oxide Nanowires/Single-Walled Carbon Nanotube Hybrid Thin Film. *ACS Nano* **2010**, *4*, 4404−4411.

(7) Cui, Y.; Lieber, C. M. Functional nanoscale electronic devices assembled using silicon nanowire building blocks. *Science* **2001**, *291*, 851−853.

(8) Chan, C. K.; Peng, H. L.; Liu, G.; Mcilwrath, K.; Zhang, X. F.; Huggins, R. A.; Cui, Y. High-performance lithium battery anodes using silicon nanowires. *Nat. Nanotechnol.* **2008**, *3*, 31−35.

(9) Yang, Y.; Jeong, S.; Hu, L. B.; Wu, H.; Lee, S. W.; Cui, Y. Transparent lithium-ion batteries. *Proc. Natl. Acad. Sci. U.S.A.* **2011**, *108*, 13013−13018.

(10) Nam, K. T.; Kim, D. W.; Yoo, P. J.; Chiang, C. Y.; Meethong, N.; Hammond, P. T.; Chiang, Y. M.; Belcher, A. M. Virus-enabled synthesis and assembly of nanowires for lithium ion battery electrodes. *Science* **2006**, *312*, 885−888.

(11) Nishide, H.; Oyaizu, K. Toward flexible batteries. *Science* **2008**, *319*, 737−738.

(12) Yang, L.; Cheng, S.; Ding, Y.; Zhu, X. B.; Wang, Z. L.; Liu, M. L. Hierarchical Network Architectures of Carbon Fiber Paper Supported Cobalt Oxide Nanonet for High-Capacity Pseudocapacitors. *Nano Lett.* **2012**, *12*, 321−325.

(13) Lee, J. S.; Park, G. S.; Lee, H. I.; Kim, S. T.; Cao, R. G.; Liu, M. L.; Cho, J. Ketjenblack Carbon Supported Amorphous Manganese Oxides Nanowires As Highly Efficient Electrocatalyst for Oxygen Reduction Reaction in Alkaline Solutions. *Nano Lett.* **2011**, *11*, 5362−5366.

(14) Scrosati, B. Nanomaterials: paper powers battery breakthrough. *Nat. Nanotechnol.* **2007**, *2*, 598−599.

(15) Rogers, J. A.; Someya, T.; Huang, Y. G. Materials and mechanics for stretchable electronics. *Science* **2010**, *327*, 1603−1607.

(16) Nyholm, L.; Nystrom, G.; Mihranyan, A.; Stromme, M. Toward flexible polymer and paper-based energy storage devices. *Adv. Mater.* **2011**, *23*, 3751−3769.

(17) Hertzberg, B.; Alexeev, A.; Yushin, G. Deformations in Si-Li Anodes upon Electrochemical Alloying in Nanoconfined Space. *J. Am. Chem. Soc.* **2010**, *132*, 8548−8549.

(18) Park, M. H.; Kim, K.; Kim, J.; Cho, J. Flexible dimensional control of high-capacity li-ion-battery anodes: from 0D hollow to 3D porous germanium nanoparticle assemblies. *Adv. Mater.* **2010**, *22*, 415−418.

(19) Seo, M. H.; Park, M.; Lee, K. T.; Kim, K.; Kimb, J.; Cho, J. High performance Ge nanowire anode sheathed with carbon for lithium rechargeable batteries. *Energy Environ. Sci.* **2011**, *4*, 425−428.

(20) Chen, H. T.; Xu, J.; Chen, P. C.; Fang, X.; Qiu, J.; Fu, Y.; Zhou, C. W. Bulk Synthesis of Crystalline and Crystalline Core/Amorphous Shell Silicon Nanowires and Their Application for Energy Storage. *ACS Nano* **2011**, *5*, 8383−8390.

(21) Jia, X. L.; Yan, C. Z.; Chen, Z.; Wang, W. W.; Zhang, Q.; Guo, L.; Wei, F.; Lu, Y. F. Direct growth of flexible $LiMn_2O_4$/CNT lithium-ion cathodes. *Chem. Commun.* **2011**, *47*, 9669−9671.

(22) Jabbour, L.; Gerbaldi, C.; Chaussy, D.; Zeno, E.; Bodoardo, S.; Beneventi, D. Microfibrillated cellulose−graphite nanocomposites for highly flexible paper-like Li-ion battery electrodes. *J. Mater. Chem.* **2010**, *20*, 7344−7347.

(23) Hu, L.; Mantia, F. L.; Wu, H.; Xie, X.; McDonough, J.; Pasta, M.; Cui, Y. Lithium-ion textile batteries with large areal mass loading. *Adv. Energy Mater.* **2011**, *1*, 1012−1017.

(24) Sharma, Y.; Sharma, N.; Rao, G.; Chowdari, B. Nanophase $ZnCo_2O_4$ as a high performance anode material for li-ion batteries. *Adv. Funct. Mater.* **2007**, *17*, 2855−2861.

(25) Qiu, Y. C.; Yang, S. H.; Deng, H.; Jin, L. M.; Li, W. S. A novel nanostructured spinel $ZnCo_2O_4$ electrode material: morphology conserved transformation from a hexagonal shaped nanodisk precursor and application in lithium ion batteries. *J. Mater. Chem.* **2010**, *20*, 4439−4444.

(26) Du, N.; Xu, Y. F.; Zhang, H.; Yu, J. X.; Zhai, C. X.; Yang, D. R. Porous $ZnCo_2O_4$ Nanowires Synthesis via Sacrificial Templates: High-Performance Anode Materials of Li-ion Batteries. *Inorg. Chem.* **2011**, *50*, 3320−3324.

(27) Deng, D.; Lee, J. Y. Linker-free 3D assembly of nanocrystals with tunable unit size for reversible lithium ion storage. *Nanotechnology* **2011**, *22*, 355401.

(28) Cui, Y.; Zhong, Z.; Wang, D.; Wang, W. U.; Lieber, C. M. High-Performance Silicon Nanowire Field Effect Transistors. *Nano Lett.* **2003**, *3*, 149−152.

(29) Niu, M. T.; Huang, F.; Cui, L. F.; Huang, P.; Yu, Y. L.; Wang, Y. S. Hydrothermal Synthesis, Structural Characteristics, and Enhanced Photocatalysis of SnO_2/alpha-Fe_2O_3 Semiconductor Nanoheterostructures. *ACS Nano* **2010**, *4*, 681−688.

(30) Liang, W. J.; Yuhas, B. D.; Yang, P. D. Magnetotransport in Co-doped ZnO Nanowires. *Nano Lett.* **2009**, *9*, 892−896.
(31) Bae, J.; Song, M. K.; Park, Y. J.; Kim, J. M.; Liu, M. L.; Wang, Z. L. Fiber supercapacitors made of nanowire-fiber hybrid structures for wearable/flexible energy storage. *Angew. Chem., Int. Ed.* **2011**, *50*, 1683−1687.
(32) Dong, Y. J.; Yu, G. H.; McAlpine, M. C.; Lu, W.; Lieber, C. M. Si/a-Si Core/Shell Nanowires As Nonvolatile Crossbar Switches. *Nano Lett.* **2008**, *8*, 386−391.
(33) Sun, Y. K.; Myung, S. T.; Park, B. C.; Prakash, J.; Belharouak, I.; Amine, K. High-energy cathode material for long-life and safe lithium batteries. *Nat. Mater.* **2009**, *8*, 320−324.
(34) Zhang, Q.; Chen, X. Y.; Zhou, Y. X.; Zhang, G. B.; Yu, S. H. Synthesis of $ZnWO_4$@MWO_4 (M = Mn, Fe) Core−Shell Nanorods with Optical and Antiferromagnetic Property by Oriented Attachment Mechanism. *J. Phys. Chem. C* **2007**, *111*, 3927−3933.
(35) Liu, J. P.; Jiang, J.; Cheng, C. W.; Li, H. X.; Zhang, J. X.; Gong, H.; Fan, H. J. Co_3O_4 nanowire@MnO_2 ultrathin nanosheet core/shell arrays: A new class of high-performance pseudocapacitive materials. *Adv. Mater.* **2011**, *23*, 2076−2081.
(36) Mai, L. Q.; Yang, F.; Zhao, Y. L.; Xu, X.; Xu, L.; Luo, Y. Z. Hierarchical $MnMoO_4$/$CoMoO_4$ heterostructured nanowires with enhanced supercapacitor performance. *Nat. Commun.* **2011**, *2*, 1−5.
(37) Hassoun, J.; Lee, K. S.; Sun, Y. K.; Scrosati, B. An Advanced Lithium Ion Battery Based on High-Performance Electrode Materials. *J. Am. Chem. Soc.* **2011**, *133*, 3139−3143.
(38) Poizot, P.; Laruelle, S.; Grugeon, S.; Dupont, L.; Tarascon, J. M. Nano-sized transition-metal oxides as negative-electrode materials for lithium-ion batteries. *Nature* **2000**, *407*, 496−499.
(39) Wang, X.; Li, X.; Sun, X.; Li, F.; Liu, Q.; Wang, Q.; He, D. Nanostructured NiO electrode for high rate Li-ion batteries. *J. Mater. Chem.* **2011**, *21*, 3571−3573.
(40) Zhou, G.; Wang, D. W.; Li, F.; Zhang, L.; Li, N.; Wu, Z. S.; Wen, L.; Lu, G. Q.; Cheng, H. M. Graphene-wrapped Fe_3O_4 anode material with improved reversible capacity and cyclic stability for lithium ion batteries. *Chem. Mater.* **2010**, *22*, 5306−5313.
(41) Grugeon, S.; Laruelle, S.; Dupont, L.; Tarascon, J. M. An update on the reactivity of nanoparticles Co-based compounds towards Li. *Solid State Sci.* **2003**, *5*, 895−904.
(42) Laruelle, S.; Grugeon, S.; Poizot, P.; Dolle, M.; Dupont, L.; Tarascon, J. M. On the origin of the extra electrochemical capacity displayed by MO/Li cells at low potential. *J. Electrochem. Soc.* **2002**, *149*, A627−A634.
(43) Li, Y. G.; Tan, B.; Wu, Y. Y. Mesoporous Co_3O_4 Nanowire Arrays for Lithium Ion Batteries with High Capacity and Rate Capability. *Nano Lett.* **2008**, *8*, 265−270.
(44) Wang, Y.; Xia, H.; Lu, L.; Lin, J. Y. Excellent Performance in Lithium-Ion Battery Anodes: Rational Synthesis of $Co(CO_3)_{0.5}(OH)$-$0.11H_2O$ Nanobelt Array and Its Conversion into Mesoporous and Single-Crystal Co_3O_4. *ACS Nano* **2010**, *4*, 1425−1432.